Emergent Non-Eulerian Hydrodynamics of Quantum Vortices in Two Dimensions

Xiaoquan Yu* and Ashton S. Bradley†
Department of Physics, Centre for Quantum Science, and Dodd-Walls Centre for Photonic and Quantum Technologies, University of Otago, Dunedin 9054, New Zealand
(Received 7 April 2017; revised manuscript received 17 August 2017; published 30 October 2017)

We develop a coarse-grained description of the point-vortex model, finding that a large number of planar vortices and antivortices behave as an inviscid non-Eulerian fluid at large scales. The emergent binary vortex fluid is subject to anomalous stresses absent from Euler's equation, caused by the singular nature of quantum vortices. The binary vortex fluid is compressible, and has an asymmetric Cauchy stress tensor allowing orbital angular momentum exchange with the vorticity and vortex density. An analytic solution for vortex shear flow driven by anomalous stresses is in excellent agreement with numerical simulations of the point-vortex model.

DOI: 10.1103/PhysRevLett.119.185301

Introduction.—Topological defects play a key role in the two-dimensional (2D) superfluid transition [1,2], and in many out of equilibrium phenomena including phase ordering dynamics after a quench [3–5] and turbulence in Bose-Einstein condensates (BECs) [6–13]. Under planar confinement [14] the collective motion of many interacting quantum vortices in a superfluid leads to the emergent complexity of 2D quantum turbulence (2DQT) [15–25]. Experimental advances now allow plane-confined BECs [26,27], and simultaneous detection of quantum vortex positions and circulations [28], opening the way to studies of 2DQT and Onsager vortices [29–36].

In the hydrodynamic regime at low temperature, superfluid vortex motion is much slower than the rate of sound propagation, and a system of many quantum vortices evolves as an almost isolated subsystem: a vortex fluid. The point-vortex model (PVM), a central model for studying 2D classical incompressible turbulent flows [29,30,37,38], describes the dynamics of quantum vortices [39,40], provided they are well separated. In this regime the vortex core structure is unimportant, and the coupling to acoustic modes is relatively weak [41]. Many studies of collective dynamics of vortices rely on large-scale numerical simulations of the discrete PVM [42–45]. An alternate approach was initiated by Wiegmann and Abanov [46], who formulated a hydrodynamic description of well-separated vortices of the same circulation, providing a rigorous starting point for studying rotating fluids, vortex clusters with a definite sign of vorticity [47,48], and the connection between vortex fluids and quantum Hall liquids [49]. A general 2D turbulent flow or a phase ordering process involves many vortices and antivortices, motivating a hydrodynamic theory of the binary vortex system.

In this Letter we develop a hydrodynamic formulation of systems involving a large number of vortices and antivortices, providing a framework for describing their emergent collective dynamics at large scales. A system containing many vortices with mean separation much bigger than the vortex core size ξ can be treated as a fluid on a scale much larger than ξ, and smaller than the system size. We generalize the coarse-graining procedure proposed for chiral vortex systems [46] to the binary vortex system by introducing two hydrodynamical velocity fields via vortex number and charge currents. The binary fluid obeys a compressible hydrodynamic equation containing an asymmetric Cauchy stress tensor and an anomalous stress that is analogous to viscous stress while conserving energy. A vortex fluid shear flow driven by the anomalous stress is found, and numerical simulations of the PVM show excellent agreement with the analytical solution. Variation of the coarse-graining scale also demonstrates convergence of many-body dynamics of the PVM to non-Eulerian hydrodynamics. Dissipation due to the interaction between vortices and the thermal cloud generates uphill diffusion of the vorticity at macroscopic scales. Chiral flow dynamics [46] is recovered as a special case of the binary fluid.

Two-dimensional hydrodynamics.—The dynamics of nonviscous incompressible classical fluids in 2D is described by the Euler equation

$$\mathcal{D}_t^u \mathbf{u} = -\frac{1}{nm}\nabla p, \qquad \nabla\cdot\mathbf{u} = 0, \tag{1}$$

where n is the constant density, $\mathbf{u}$ is the fluid velocity, $\mathcal{D}_t^u \equiv \partial_t + \mathbf{u}\cdot\nabla$ is the material derivative with respect to $\mathbf{u}$, m is the atomic mass, and p is the fluid pressure determined by $\nabla\cdot(\mathbf{u}\cdot\nabla\mathbf{u}) = -(nm)^{-1}\nabla^2 p$. Taking the curl of Eq. (1), the Helmholtz equation for the vorticity $\omega \equiv [\nabla\times\mathbf{u}]_z$ is

$$\mathcal{D}_t^u \omega = 0. \tag{2}$$

The kinetic energy of the fluid reads [50]

$$H = \frac{nm}{2}\int d^2\mathbf{r}|\mathbf{u}|^2 = \frac{nm}{2}\int d^2\mathbf{r}\psi(\mathbf{r})\omega(\mathbf{r}), \tag{3}$$

where ψ is the stream function, and $\mathbf{u} = \nabla\times(\psi\hat{\mathbf{z}})$ and $-\nabla^2\psi = \omega$. Here, $\hat{\mathbf{z}}$ is a unit normal vector to the fluid plane.

For a 2D flow, it is convenient to use complex coordinates $z = x + iy$, $\partial_z = (\partial_x - i\partial_y)/2$ and the complex velocity $u = u_x - iu_y$. In terms of complex notation $\nabla \cdot \mathbf{u} = \partial_z \bar{u} + \partial_{\bar{z}} u$, $\mathbf{u} \cdot \nabla = \bar{u}\partial_z + u\partial_{\bar{z}}$, $\omega = [\nabla \times \mathbf{u}]_z = i(\partial_{\bar{z}} u - \partial_z \bar{u}) = 2i\partial_{\bar{z}} u$, and $u = 2i\partial_z \psi$. We also use subscripts a, b to denoted the Cartesian components of vectors, and use vector, complex, or component notation where convenient.

Point-vortex system.—A superfluid containing vortices with a separation larger than the core size ξ is nearly incompressible, away from vortex cores [51]. For a BEC described by a macroscopic wave function Ψ, the associated Gross-Pitaevskii equation (GPE) governing time evolution can be mapped to the form of Eq. (1) in the incompressible regime (constant density $n = |\Psi|^2$) [52,53]. The single valuedness of the wave function Ψ requires that the circulation of a vortex excitation must be quantized in units of circulation quantum $\kappa \equiv 2\pi\hbar/m$, and the vorticity has a singularity at the position of the vortex core $\mathbf{r}_i$: $\omega(\mathbf{r}) = \kappa\sigma_i\delta(\mathbf{r} - \mathbf{r}_i)$ with the sign $\sigma_i = \pm 1$. Hereafter, we set $nm = 1$ for convenience.

We consider a system containing N_+ singly charged quantum vortices and N_- antivortices. The total number of vortices is $N = N_+ + N_-$ and the vortex with sign σ_i is located at $\mathbf{r}_i$. The fluid velocity generated by these quantum vortices far from the fluid boundary is completely determined by the vorticity: $u = 2i\partial_z\psi = (2\pi i)^{-1}\int d^2\mathbf{r}'\omega(\mathbf{r}')/(z - z') = -\sum_{j=1}^N i\gamma\sigma_j/(z - z_j)$, where the stream function of the fluid is $\psi(\mathbf{r}) = -\gamma\sum_i \sigma_i \log|(\mathbf{r} - \mathbf{r}_i)/\ell|$, and the vorticity is $\omega(\mathbf{r}) = 2\pi\gamma\sum_i\sigma_i\delta(\mathbf{r} - \mathbf{r}_i)$. Here, ℓ is a length scale introduced to ensure the correct dimension, and $\gamma = \kappa/2\pi$ is a convenient unit of circulation. As shown by Helmholtz, the above fluid velocity u is a singular solution of Eq. (2). A quantum vortex generates a flow in the bulk fluid, while the vortex core is a pointlike particle and has its own dynamics driven by the flow generated by the other vortices. The dynamics of the vortex cores has a Hamiltonian structure:

$$\frac{dz_i}{dt} = \frac{\partial \mathcal{H}}{\partial p_i}, \qquad \frac{dp_i}{dt} = -\frac{\partial \mathcal{H}}{\partial z_i} \tag{4}$$

with canonical momentum $p_i = i\pi\gamma\sigma_i\bar{z}_i$ and Hamiltonian

$$\mathcal{H} = -\pi\gamma^2\sum_{i\neq j}\sigma_i\sigma_j\log\left|\frac{z_i - z_j}{\ell}\right|. \tag{5}$$

The formal solutions of Eq. (4) are the Kirchhoff equations [54]

$$\frac{d\bar{z}_i}{dt} = v_i, \qquad v_i = -\sum_{j,j\neq i}^{N}\frac{i\gamma\sigma_j}{z_i(t) - z_j(t)}. \tag{6}$$

Using the vortex degrees of freedom, the kinetic energy of the fluid $H = \mathcal{H} + E_{\mathrm{self}}$, where $\mathcal{H}$ is the energy of interaction between vortices, and $E_{\mathrm{self}} = N\pi\gamma^2\log(\ell/\xi)$ is the total self-energy. The PVM can be seen as a limiting case of the vortex method [55,56] and well approximates incompressible classical fluids with κ determined by the injection scale.

Vortex fluid hydrodynamics.—For large N, the emergent collective dynamics of the discrete vortex system [Eq. (6)] can be described by a few hydrodynamic variables. By coarse-graining microscopic vortex distributions over patches containing many vortices, we derive a hydrodynamic formulation of the PVM, describing the vortex dynamics on scales greater than the patch scale. The core size ξ is much smaller than the patch scale, and serves as a natural ultraviolet cutoff.

Under Hamiltonian evolution, conservation laws ensure the following continuity equations

$$\partial_t\rho = \sum_i\partial_t\delta(\mathbf{r} - \mathbf{r}_i(t)) = -(\partial_z\bar{J}_n + \partial_{\bar{z}}J_n) = -\nabla\cdot\mathbf{J}_n, \tag{7}$$

$$\partial_t\sigma = \sum_i\sigma_i\partial_t\delta(\mathbf{r} - \mathbf{r}_i(t)) = -(\partial_z\bar{J}_c + \partial_{\bar{z}}J_c) = -\nabla\cdot\mathbf{J}_c, \tag{8}$$

where the vortex number density $\rho(\mathbf{r}) \equiv \sum_i\delta(\mathbf{r} - \mathbf{r}_i)$, the vortex charge density $\sigma(\mathbf{r}) \equiv \sum_i\sigma_i\delta(\mathbf{r} - \mathbf{r}_i) = (2\pi\gamma)^{-1}\omega$, and

$$J_c = \sum_i\delta(\mathbf{r} - \mathbf{r}_i)(\sigma_i v_i), \qquad J_n = \sum_i\delta(\mathbf{r} - \mathbf{r}_i)v_i \tag{9}$$

are the currents for charge and number, respectively. The coarse-grained vortex charge velocity field w and vortex velocity field v are defined according to the hydrodynamic relations $J_c \equiv \rho w$ and $J_n \equiv \rho v$ [57]. Using the identity

$$2\sum_{i\neq j}\frac{\sigma_i}{z - z_i}\frac{\sigma_j}{z_i - z_j} = \left(\sum_i\frac{\sigma_i}{z - z_i}\right)^2 + \partial_z\sum_i\frac{1}{z - z_i} \tag{10}$$

with Eq. (6), we can rewrite J_c to obtain an important relation between the vortex charge velocity w, and the fluid velocity u, given by

$$\rho w = \sigma u - 2\eta i\partial_z\rho \tag{11}$$

with anomalous kinetic coefficient $\eta = \gamma/4$; here we have used $\partial_{\bar{z}}(1/z) = \pi\delta(\mathbf{r})$ and $[\partial_z, \partial_{\bar{z}}](1/z) = 0$. A fundamental relation linking the vortex velocity field v to the fluid velocity u can also be derived by decomposing J_n [58], to give

$$\rho v = \rho u - 2i\eta\partial_z\sigma. \tag{12}$$

The two velocity fields are related by

$$\rho w = \sigma v - i\eta\rho^{-1}(\partial_z\rho^2 - \partial_z\sigma^2), \tag{13}$$

and the vorticity of the vortex velocity field v, $\omega_v \equiv i(\partial_{\bar{z}}v - \partial_z\bar{v})$, has the anomalous correction

$$\omega_v - \omega = \nabla \times (\mathbf{v} - \mathbf{u}) = \eta \nabla \cdot (\rho^{-1} \nabla \sigma). \qquad (14)$$

In the hydrodynamic formulation the quantities ρ, σ, J_c, and J_n represent averages of the corresponding microscopic quantities over patches, giving smooth coarse-grained quantities on the patch scale [59].

The relation (12) links the superfluid velocity field that is irregular at a vortex core to a vortex fluid velocity field that is regular. In other words, the velocity of a vortex at position $\mathbf{r}$ is the fluid velocity excluding the flow generated by the vortex itself at $\mathbf{r}$. The regularization involves subtracting the singular term, namely, the pole at the vortex core. For a single vortex at the origin the superfluid velocity $u = -i\gamma\sigma_i/z$ and $2i\eta\partial_z\sigma/\rho = -4i\eta\sigma_i/z$; Eq. (12) yields $v = u - 2i\eta\partial_z\sigma/\rho = 0$. The correction cancels out the superfluid velocity field due to the local vortex, giving the physical result that a vortex does not move under the action of its own velocity field. Equation (11) has a similar interpretation.

The binary vortex fluid is compressible:

$$\nabla \cdot \mathbf{v} = 2\eta i[\partial_z(\rho^{-1}\partial_{\bar{z}}\sigma) - \mathrm{H.c.}] = -\eta \nabla \times (\rho^{-1}\nabla\sigma) \neq 0, \qquad (15)$$

as also seen from $\nabla \cdot \mathbf{w} = \bar{u}\partial_z(\sigma/\rho) + u\partial_{\bar{z}}(\sigma/\rho) \neq 0$. In the chiral limit, $\sigma = \rho$, $w = v$ and $\nabla \cdot \mathbf{v} = 0$ [46]. The chiral vortex fluid is rigid, as the energy cost to compress a vortex fluid containing N vortices scales as N^2 due to repulsive interactions between like-sign vortices. For a binary vortex fluid, the presence of two opposite sign vortices softens the vortex fluid such that gapless excitations can occur, making the vortex fluid compressible.

Anomalous Euler equation.—Using Eqs. (8), (13), (15), σ satisfies the vortex fluid Helmholtz equation

$$\mathcal{D}_t^v \sigma = 0, \qquad (16)$$

and vortex charge is conserved, moving with the vortex velocity; use of Eq. (12) shows consistency with Helmholtz' equation for the fluid, Eq. (2). A straightforward calculation [58] yields the anomalous Euler equation of the vortex velocity field v

$$\partial_t(\rho v) + \partial_z \mathcal{T}_{z\bar{z}} + \partial_{\bar{z}}\mathcal{T} + \rho\partial_z(2p) = 0, \qquad (17)$$

where $\mathcal{T}_{z\bar{z}} = \rho v\bar{v} + 16\eta^2\pi\sigma^2 + 4\eta^2\sigma\partial_{\bar{z}}(\rho^{-1}\partial_z\sigma)$ and $\mathcal{T} = \rho vv + 4\eta^2\sigma\partial_z(\rho^{-1}\partial_z\sigma) - 4\eta i\sigma\partial_z v$ are complex components of the momentum flux tensor. Equation (17) does not explicitly contain w and Eqs. (7), (16), and (17) fully describe the binary vortex fluid. In Cartesian coordinates Eq. (17) becomes

$$\partial_t(\rho v_a) + \partial_b \mathcal{T}_{ab} + \rho\partial_a p = 0, \qquad (18)$$

where the momentum flux tensor $\mathcal{T}_{ab} = \rho v_a v_b - \Pi_{ab}$ [61] with the emergent Cauchy stress tensor

$$\Pi_{ab} = -\sigma\tau_{ab} - 8\eta^2\pi\sigma^2\delta_{ab} - \eta^2\sigma\partial_b(\rho^{-1}\partial_a\sigma), \qquad (19)$$

reflecting the macroscopic effects of the topological nature of quantum vortices. The anomalous stress

$$\tau_{xy} = \tau_{yx} = \eta(\partial_x v_x - \partial_y v_y),$$
$$\tau_{xx} = -\tau_{yy} = -\eta(\partial_x v_y + \partial_y v_x) \qquad (20)$$

does not cause energy dissipation and is formally identical to that of the chiral vortex fluid [46]. The anomalous stress τ_{ab} vanishes in uniform rotation with angular velocity Ω, where $v = -\Omega i\bar{z}$. Although there is no frictional viscosity in the binary vortex fluid, the shear stress ($\Pi_{ab} \neq 0$ for $a \neq b$) is nonvanishing, induced by gradients of ρ and σ and the anomalous stress τ_{ab}. A similar situation can be found in the GPE when quantum pressure is important [62].

A conspicuous feature of the Cauchy stress tensor Π_{ab} for the binary vortex fluid is that it is asymmetric, with a nontrivial commutator linking to the compressibility

$$\Pi_{xy} - \Pi_{yx} = -\sigma\eta\nabla \cdot \mathbf{v}. \qquad (21)$$

Note that under the transformation $x \leftrightarrow y$, the velocity $v_x \to -v_y$ and $v_y \to -v_x$, and hence $\nabla \cdot \mathbf{v} \to -\nabla \cdot \mathbf{v}$. For the chiral fluid $\sigma = \rho$, $\nabla \cdot \mathbf{v} = 0$ and Π_{ab} is symmetric [46]. The local mechanical pressure of the binary vortex fluid is given by the normal stress:

$$p_m = -\frac{1}{2}\mathrm{tr}(\Pi_{ab}) = 8\eta^2\pi\sigma^2 + \frac{1}{2}\eta^2\sigma\nabla \cdot (\rho^{-1}\nabla\sigma). \qquad (22)$$

Angular momentum.—The canonical angular momentum of the point-vortex system that is associated with rotational symmetry reads $L^c \equiv \sum_i^N \mathbf{r}_i \times \mathbf{p}_i = -\pi\gamma\sum_i \sigma_i r_i^2$, and is equivalent to the fluid angular momentum $L_f = \int d^2\mathbf{r}\mathbf{r} \times \mathbf{u} = -1/2\int d^2\mathbf{r} r^2\omega$. The canonical angular momentum L^c is conserved as long as the system has rotational symmetry. We can also consider the orbital angular momentum (OAM) of vortices $L^v \equiv \sum_i^N \mathbf{r}_i \times \mathbf{v}_i$. For a chiral vortex system ($\sigma_i = 1$), $L^v = 2\eta N(N-1)$. In terms of the hydrodynamic field v, $L^v = \int d^2\mathbf{r}\mathcal{L}^v$ with $\mathcal{L}^v = \mathbf{r} \times (\rho\mathbf{v})$. In Cartesian coordinates $\mathcal{L}_{ab}^v = \rho(x_a v_b - x_b v_a)$. Using Eq. (18), we obtain the continuity equation

$$\frac{\partial \mathcal{L}_{ab}^v}{\partial t} + \partial_c \mathcal{M}_{abc} = \Pi_{ba} - \Pi_{ab} \qquad (23)$$

with angular momentum flux tensor $\mathcal{M}_{abc} = x_a\mathcal{T}_{bc} - x_b\mathcal{T}_{ac}$, indicating that the OAM is conserved if and only if $\Pi_{ab} = \Pi_{ba}$. Since Π_{ab} is asymmetric for the binary vortex fluid, the OAM is not conserved regardless of the symmetry, consistent with the property of the corresponding discrete point-vortex system [63]. For the incompressible chiral vortex fluid ($\nabla \cdot \mathbf{v} = 0$), the OAM is conserved. The divergence $\nabla \cdot \mathbf{v}$ is a source term in Eq. (23), and η can be seen as a rotational viscous coefficient mediating the exchange between the vortex fluid OAM and the internal vorticity and density degrees of freedom. The conserved OAM of the binary point-vortex system can be constructed by considering the sign-weighted OAM $L^w \equiv \sum_i^N \mathbf{r}_i \times (\sigma_i \mathbf{v}_i) = 2\eta[(\sum_i \sigma_i)^2 - N]$. In the chiral case $L^w = L^v$ and $L^w = -2\eta N$ for the neutral system; in terms of w, $L^w = \int d^2\mathbf{r}\mathbf{r} \times (\rho\mathbf{w})$.

Vortex fluid Hamiltonian.—Since $\sigma_i v_i \propto dp_i/dt$ and $\sum_i \delta(\mathbf{r}-\mathbf{r}_i)\partial\mathcal{H}/\partial z_i = \sum_i \delta(\mathbf{r}-\mathbf{r}_i)\sigma_i v_i$, the vortex charge velocity w satisfies the canonical equation $-i\pi\gamma\rho w = \sigma\partial_z(\delta\mathcal{H}[\rho,\sigma]/\delta\sigma) + \rho\partial_z(\delta\mathcal{H}[\rho,\sigma]/\delta\rho)$, which gives the Hamiltonian of the binary vortex fluid [64]

$$\mathcal{H}[\rho,\sigma] = H[\sigma] - 8\pi\eta^2 \int d^2\mathbf{r}\rho\log(\ell^2\rho). \tag{24}$$

Here, $H[\sigma]$ is the fluid Hamiltonian (3), and the second term is the self-energy of vortices [65]. The Hamiltonian (24) is the hydrodynamic formulation to the discrete point-vortex Hamiltonian (5). It can be decomposed as $\mathcal{H}[\rho,\sigma] = H_{\rm kin} + H_{\rm int} + H_{\rm so}$ with vortex fluid kinetic energy $H_{\rm kin} = 1/2\int d^2\mathbf{r}|\mathbf{v}|^2$, "internal energy" $H_{\rm int} = \eta^2/2\int d^2\mathbf{r}(\rho^{-2}|\nabla\sigma|^2 - 16\pi\rho\log(\ell^2\rho))$, and a "spin-orbit coupling" term $H_{\rm so} = -\eta\int d^2\mathbf{r}\rho^{-1}\mathbf{v}\cdot(\hat{z}\times\nabla\sigma)$ that couples vortex distribution energy to vortex fluid kinetic energy.

Vortex shear flows.—We consider a static vortex flow with $v_y = 0$, $\partial_x v_x = 0$, and $\partial_x\sigma = 0$ in a neutral vortex system of constant density $\rho = \rho_0$. For such a static flow Eq. (18) reduces to $\partial_b\mathcal{T}_{ab} = \partial_b(\rho_0 v_a v_b - \Pi_{ab}) = \partial_b\Pi_{ab} = 0$ [66], where the only nontrivial component reads $(\partial_y\sigma\partial_y + \sigma\partial_y^2)v_x + \eta[16\pi\sigma\partial_y + \rho_0^{-1}(\partial_y\sigma\partial_y^2 + \sigma\partial_y^3)]\sigma = 0$, indicating that $\mathbf{v}$ is completely determined by the emergent Cauchy stress tensor including the anomalous stress τ_{ab}. An exact shear flow solution to Eq. (18) can then be found:

$$\sigma(x,y) = \sigma_0\sin(\alpha y), \qquad \mathbf{v} = (v_0\cos(\alpha y), 0), \tag{25}$$

where $v_0 = \alpha\eta\sigma_0(8\pi\alpha^{-2} - \rho_0^{-1})$, and α is a real parameter. Numerical simulations of the PVM with $N = 9522$ [67] in a doubly periodic square box with side length $L = 6\times 10^3\xi$ [68] show excellent agreement with the prediction of Eq. (25) (see Fig. 1). Good agreement is also seen for $N = 450$ and $L = 300\xi$, being nearly within reach of current BEC experiments [21,26,27]. There may also be more exotic vortex flows with an enhanced anomalous term in Eq. (12), as may be caused by a gradient discontinuity in σ.

Dissipation and annihilation.—To model dissipation due to interaction between superfluid vortices and a noncondensed thermal cloud [71], we consider a dissipative point-vortex model [24,72–74] of the form $d\bar{z}_i/dt = v_i + i\eta^*\sigma_i v_i$ [75], where the dimensionless dissipation rate η^* measures energy damping [78]. In the presence of dissipation, the continuity equations (7) and (8) still hold subject to the substitutions $\mathbf{J}_n \to \mathbf{J}'_n = \mathbf{J}_n - \eta^*\hat{\mathbf{z}}\times\mathbf{J}_c$ and $\mathbf{J}_c \to \mathbf{J}'_c = \mathbf{J}_c - \eta^*\hat{\mathbf{z}}\times\mathbf{J}_n$. The dissipative Helmholtz equation is $\mathcal{D}_t^{\hat{v}}\sigma = -\eta^*(8\pi\eta\rho\sigma + \eta\nabla^2\sigma - \mathbf{v}\times\nabla\rho)$, where $\hat{\mathbf{v}} \equiv \mathbf{v} - \eta^*\eta\nabla\log\rho$; the terms $-8\pi\eta\eta^*\rho\sigma$ and $\eta^*\mathbf{v}\times\nabla\rho$ describe damping and transverse damping, respectively. The negative sign in front of the diffusion term induces uphill diffusion of σ, concentrating vorticity, and may contribute to inverse energy cascades and vortex clustering processes [24,44].

Various forms of vortex number loss can modify the Hamiltonian theory, including vortex annihilations due to collisions, and dissipative vortex dipole decay or boundary loss. For a low temperature BEC containing many vortices the dissipation rate is small, $\eta^* \simeq 10^{-4}$ [18], and annihilations due to collisions are the dominant limitation for the Hamiltonian PVM approach. However, their influence is regime dependent [79] and can be negligible for highly vorticity-polarized states, examples of which are the vortex shear flow (see Fig. 1) [87], the enstrophy cascade in decaying 2DQT [45], and Onsager clustered states [25,33,88]. In the vortex dipole gas regime, dipole-dipole collisions are frequent and the theory is valid for times shorter than the dipole lifetime. The characteristic quantities are the collision cross section $\sigma_{\rm cs} \sim \xi$, the root-mean-square dipole velocity $v_{\rm rms} \sim \kappa d^{-1}$ (for $d \lesssim 10\xi$ the Jones-Roberts soliton [89,90] forms), the mean free path $\ell_m \sim (\sigma_{\rm cs}\rho_d)^{-1}$, and the mean free time $\tau = \ell_m/v_{\rm rms} \sim 10/(\kappa\rho_d)$, where $\rho_d = \rho/2$ is the dipole density. The average total collision frequency per unit area is then $\tau^{-1}\rho_d$, and assuming that every collision annihilates two vortices, we find the rate equation $dN/dt = -\Gamma_2 N^2$, where the two-body decay rate

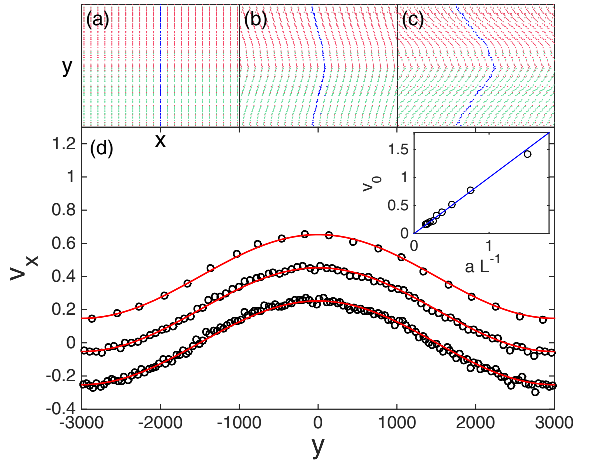

FIG. 1. The initial vortex configuration is obtained by sampling vortex coordinates according to the distribution $\sigma = \sigma_0\sin(2\pi y/L)$ with $y\in[-L/2, L/2]$, and $\sigma_0 = \rho_0$. We measure length L, velocity v, and time t in units of ξ, κ/ξ, and ξ^2/κ, respectively. Panels (a), (b), and (c) show the evolution of point vortices (red: $\sigma_i = 1$; green: $\sigma_i = -1$) at $t = 0$, 50, 150, respectively. In each plot, x and y range from -10^3 to 10^3 and -3×10^3 to 3×10^3. The 138 vortices initially located at $x = 0$ are labeled blue and their velocities are used to characterize the shear flow. (d) Comparison between Eq. (25) (red) and simulations (circles). Velocities of the blue colored vortices are obtained as averages over ten runs (bottom). By averaging the velocities over the increasing bin size $L/\{138, 80, 20\}$ (from bottom to top), the coarse-grained vortex velocities approach the analytical result (25). For clarity the results for different bin sizes are vertically shifted by 0.2. The inset in panel (d) shows the estimated values (circles) of v_0 via fitting to the numerical data in a single run for each $L\in\{1,2,\ldots,10\}\times 10^3$, where $a = N/2\pi - 1/4$; also shown is the analytical result (blue). In our sampling the constant density is anisotropic, with the density along the y axis twice that of the density along the x axis.

$\Gamma_2 = 2\tau^{-1}\rho_d A$ and A is the system area. Such a decay behavior has recently been reported [21]; using their experimental parameters we estimate $\Gamma_2 \simeq 0.054\ \mathrm{s}^{-1}$, close to the rate observed for the highest temperature. For the same parameters, the Hamiltonian PVM is a valid description up to the mean free time (lifetime) of a dipole, $\tau \sim 300$ ms [91]. For regimes at higher vortex energy than the dipole gas limit, the decay rate per vortex can be strongly suppressed [33]. Including vortex-antivortex annihilations into the hydrodynamic theory systematically is an important direction to explore in the future.

Conclusion.—Our hydrodynamical formulation of the point-vortex model reveals that the collective motion of many vortices emerges as a binary vortex fluid with rich phenomenology including an asymmetric Cauchy stress tensor and compressible flow. Examples of the former are relatively rare, and are associated with interactions between internal degrees of freedom and the bulk fluid flow, as occurs in liquid crystals [95]. Excellent agreement between the analytic solution for vortex shear flow and the numerical simulations demonstrates the validity of the coarse-grained approach to collective vortex motion. The compressible vortex fluid may support density waves; however, global plane waves appear as excitations on top of nontrivial static background flows and are thus likely to be transient in general. The hydrodynamic theory suggests many areas for exploration including local density and vorticity excitations, regular vortex flows, connections with classical flows, and states of fully developed two-dimensional quantum turbulence.

We acknowledge M. T. Reeves, B. P. Anderson, P. B. Blakie, Giulio Giusteri, L. A. Toikka, L. Williamson, and J. M. Floryan for useful discussions. We are grateful to P. Wiegmann and A. G. Abanov for helpful feedback on an earlier version of the manuscript. A. S. B. is supported by a Rutherford Discovery Fellowship administered by the Royal Society of New Zealand.

*xiaoquan.yu@otago.ac.nz
†ashton.bradley@otago.ac.nz

[1] J. M. Kosterlitz and D. J. Thouless, J. Phys. C **5**, L124 (1972).
[2] J. M. Kosterlitz and D. J. Thouless, J. Phys. C **6**, 1181 (1973).
[3] A. Bray, Adv. Phys. **43**, 357 (1994).
[4] M. Mondello and N. Goldenfeld, Phys. Rev. A **42**, 5865 (1990).
[5] A. J. Bray, A. J. Briant, and D. K. Jervis, Phys. Rev. Lett. **84**, 1503 (2000).
[6] C. F. Barenghi, R. J. Donnelly, and W. Vinen, *Quantized Vortex Dynamics and Superfluid Turbulence* (Springer Science & Business Media, New York, 2001), Vol. 571.
[7] W. Vinen, J. Low Temp. Phys. **145**, 7 (2006).
[8] C. F. Barenghi, L. Skrbek, and K. R. Sreenivasan, Proc. Natl. Acad. Sci. U.S.A. **111**, 4647 (2014).
[9] M. C. Tsatsos, P. E. S. Tavares, A. Cidrim, A. R. Fritsch, M. A. Caracanhas, F. E. A. dos Santos, C. F. Barenghi, and V. S. Bagnato, Phys. Rep. **622**, 1 (2016).
[10] N. Navon, A. L. Gaunt, R. P. Smith, and Z. Hadzibabic, Nature (London) **539**, 72 (2016).
[11] B. P. Anderson, Nature (London) **539**, 36 (2016).
[12] M. Tsubota, K. Fujimoto, and S. Yui, J. Low Temp. Phys. **188**, 119 (2017).
[13] E. A. L. Henn, J. A. Seman, G. Roati, K. M. F. Magalhães, and V. S. Bagnato, Phys. Rev. Lett. **103**, 045301 (2009).
[14] In a BEC, vortex bending can be significantly suppressed by trap confinement without destroying phase coherence, inducing effective two-dimensional vortex motion [16].
[15] R. Numasato, M. Tsubota, and V. S. L'vov, Phys. Rev. A **81**, 063630 (2010).
[16] T. W. Neely, A. S. Bradley, E. C. Samson, S. J. Rooney, E. M. Wright, K. J. H. Law, R. Carretero-González, P. G. Kevrekidis, M. J. Davis, and B. P. Anderson, Phys. Rev. Lett. **111**, 235301 (2013).
[17] M. T. Reeves, B. P. Anderson, and A. S. Bradley, Phys. Rev. A **86**, 053621 (2012).
[18] A. S. Bradley and B. P. Anderson, Phys. Rev. X **2**, 041001 (2012).
[19] P. M. Chesler, H. Liu, and A. Adams, Science **341**, 368 (2013).
[20] T. W. Neely, E. C. Samson, A. S. Bradley, M. J. Davis, and B. P. Anderson, Phys. Rev. Lett. **104**, 160401 (2010).
[21] W. J. Kwon, G. Moon, J.-Y. Choi, S. W. Seo, and Y.-I. Shin, Phys. Rev. A **90**, 063627 (2014).
[22] G. W. Stagg, A. J. Allen, N. G. Parker, and C. F. Barenghi, Phys. Rev. A **91**, 013612 (2015).
[23] M. T. Reeves, T. P. Billam, B. P. Anderson, and A. S. Bradley, Phys. Rev. Lett. **110**, 104501 (2013).
[24] T. P. Billam, M. T. Reeves, and A. S. Bradley, Phys. Rev. A **91**, 023615 (2015).
[25] A. Skaugen and L. Angheluta, Phys. Rev. E **93**, 032106 (2016).
[26] L. Chomaz, L. Corman, T. Bienaimé, R. Desbuquois, C. Weitenberg, S. Nascimbène, J. Beugnon, and J. Dalibard, Nat. Commun. **6**, 6162 (2015).
[27] G. Gauthier, I. Lenton, N. M. Parry, M. Baker, M. J. Davis, H. Rubinsztein-Dunlop, and T. W. Neely, Optica **3**, 1136 (2016).
[28] S. W. Seo, B. Ko, J. H. Kim, and Y. Shin, Sci. Rep. **7**, 4587 (2017).
[29] L. Onsager, Il Nuovo Cimento (1943-1954) **6**, 279 (1949).
[30] G. L. Eyink and K. R. Sreenivasan, Rev. Mod. Phys. **78**, 87 (2006).
[31] G. Joyce and D. Montgomery, J. Plasma Phys. **10**, 107 (1973).
[32] D. Montgomery and G. Joyce, Phys. Fluids **17** (1974).
[33] T. P. Billam, M. T. Reeves, B. P. Anderson, and A. S. Bradley, Phys. Rev. Lett. **112**, 145301 (2014).
[34] T. Simula, M. J. Davis, and K. Helmerson, Phys. Rev. Lett. **113**, 165302 (2014).
[35] X. Yu, T. P. Billam, J. Nian, M. T. Reeves, and A. S. Bradley, Phys. Rev. A **94**, 023602 (2016).
[36] A. J. Groszek, T. P. Simula, D. M. Paganin, and K. Helmerson, Phys. Rev. A **93**, 043614 (2016).
[37] E. Novikov, Zh. Eksp. Teor. Fiz. **68**, 1868 (1975).

[38] H. Aref, P. Boyland, M. Stremler, and D. Vainchtein, in *Fundamental Problematic Issues in Turbulence* (Springer, New York, 1999), pp. 151–161.
[39] A. L. Fetter, Phys. Rev. **162**, 143 (1967).
[40] F. D. M. Haldane and Y.-S. Wu, Phys. Rev. Lett. **55**, 2887 (1985).
[41] A. Lucas and P. Surówka, Phys. Rev. A **90**, 053617 (2014).
[42] R. Numasato and M. Tsubota, J. Low Temp. Phys. **158**, 415 (2010).
[43] E. D. Siggia and H. Aref, Phys. Fluids **24**, 171 (1981).
[44] A. Skaugen and L. Angheluta, Phys. Rev. E **95**, 052144 (2017).
[45] M. T. Reeves, T. P. Billam, X. Yu, and A. S. Bradley, arXiv:1702.04445.
[46] P. Wiegmann and A. G. Abanov, Phys. Rev. Lett. **113**, 034501 (2014).
[47] R. A. Smith, Phys. Rev. Lett. **63**, 1479 (1989).
[48] R. A. Smith and T. M. ONeil, Phys. Fluids B **2**, 2961 (1990).
[49] P. B. Wiegmann, Phys. Rev. B **88**, 241305 (2013).
[50] We assume that the flow vanishes at the boundaries.
[51] In this regime the Mach number $M \equiv |\mathbf{u}|/c \ll 1$, where c is the speed of sound.
[52] L. Pitaevskii and S. Stringari, *Bose-Einstein Condensation and Superfluidity* (Oxford University Press, New York, 2016), Vol. 164.
[53] In this case, the pressure $p = gn^2/2$, where g is the interaction coupling constant in the GPE
[54] G. Kirchoff, *Lectures on Mathematical Physics, Mechanics* (Teubner, Leipzig, 1877).
[55] A. J. Chorin, *Vorticity and Turbulence* (Springer Science & Business Media, New York, 1994), Vol. 103.
[56] C. Marchioro and M. Pulvirenti, *Mathematical Theory of Incompressible Nonviscous Fluids* (Springer Science & Business Media, New York, 2012), Vol. 96.
[57] This choice of density-weighted velocity fields is essential, avoiding the pathological velocity field where $\sigma = 0$. For instance, one may define $J_c = \sigma w'$ and w' is ill defined when $\sigma = 0$. As the coordinates (x, y) of a vortex are conjugate variables, Eq. (8) is recognised as the Liouville equation of the point-vortex system.
[58] See Supplemental Material at http://link.aps.org/supplemental/10.1103/PhysRevLett.119.185301 for the detailed derivation.
[59] See Supplemental Material at http://link.aps.org/supplemental/10.1103/PhysRevLett.119.185301 for the detailed explanation, which includes Ref. [60].
[60] J. D. Jackson, *Classical Electrodynamics* (John Wiley & Sons, New York, 2007).
[61] L. Landau and E. Lifshitz, *Fluid Mechanics: Landau and Lifshitz: Course of Theoretical Physics*, Vol. 6 (Elsevier, New York, 2013).
[62] T. Winiecki, B. Jackson, J. F. McCann, and C. S. Adams, J. Phys. B **33**, 4069 (2000).
[63] See Supplemental Material at http://link.aps.org/supplemental/10.1103/PhysRevLett.119.185301 for an example of a binary vortex system containing three vortices.
[64] Note that the vortex velocity field v is not a canonical variable and hence it does not have a simple canonical relation to the vortex fluid Hamiltonian.
[65] Plugging $\rho = \sum_j \delta(\mathbf{r} - \mathbf{r}_j)$ into the last term of Eq. (24), we obtain $-8\pi\eta^2 \int d^2\mathbf{r}\rho \log(\ell^2\rho) = -(1/2)\pi\gamma^2 \sum_i \log[\ell^2 \sum_j \delta(\mathbf{r}_i - \mathbf{r}_j)] \simeq -(N/2)\pi\gamma^2 \log(\ell^2/\xi^2) = N\pi\gamma^2 \log(\xi/\ell) = -E_{\text{self}}$.
[66] For such a flow, using Eq. (12) one can show that $\nabla\cdot(\mathbf{u}\cdot\nabla\mathbf{u}) = -\nabla^2 p = 0$, having a solution that solves $\partial_a p = 0$.
[67] A relatively large number of vortices ensures that a good statistics of the sampling can be achieved.
[68] See Supplemental Material at http://link.aps.org/supplemental/10.1103/PhysRevLett.119.185301 for details of simulations, which includes Refs. [45,70,71].
[69] L. Pismen, Vortices in Nonlinear Fields, *International Series of Monographs on Physics* (Clarendon Press, Oxford, 1999).
[70] J. B. Weiss and J. C. McWilliams, Phys. Fluids A: Fluid Dyn. **3**, 835 (1991).
[71] B. Jackson, N. P. Proukakis, C. F. Barenghi, and E. Zaremba, Phys. Rev. A **79**, 053615 (2009).
[72] S. Rica and E. Tirapegui, Phys. Rev. Lett. **64**, 878 (1990).
[73] O. Törnkvist and E. Schröder, Phys. Rev. Lett. **78**, 1908 (1997).
[74] G. Moon, W. J. Kwon, H. Lee, and Y.-i. Shin, Phys. Rev. A **92**, 051601 (2015).
[75] Note that this velocity-dependent dissipation does not account for vortex-sound interactions, which are acceleration dependent [76,77].
[76] W. F. Vinen, Phys. Rev. B **64**, 134520 (2001).
[77] C. F. Barenghi, N. Parker, N. Proukakis, and C. Adams, J. Low Temp. Phys. **138**, 629 (2005).
[78] Such a damping term is inherited from the damped GPE [18] due to Bose-stimulated inelastic collisions between the condensate and noncondensed thermal cloud.
[79] Including annihilations requires knowledge of vortex kinetics that are regime dependent [21,34,80–86]
[80] V. Ambegaokar, B. I. Halperin, D. R. Nelson, and E. D. Siggia, Phys. Rev. B **21**, 1806 (1980).
[81] J. Schole, B. Nowak, and T. Gasenzer, Phys. Rev. A **86**, 013624 (2012).
[82] A. Forrester, H.-C. Chu, and G. A. Williams, Phys. Rev. Lett. **110**, 165303 (2013).
[83] C. Sire and P.-H. Chavanis, Phys. Rev. E **61**, 6644 (2000).
[84] V. Yakhot and J. Wanderer, Phys. Rev. Lett. **93**, 154502 (2004).
[85] G. F. Carnevale, J. C. McWilliams, Y. Pomeau, J. B. Weiss, and W. R. Young, Phys. Rev. Lett. **66**, 2735 (1991).
[86] M. Karl and T. Gasenzer, New J. Phys. **19**, 093014 (2017).
[87] In our simulations, annihilations are modeled phenomenologically by removing vortex dipoles with a separation less than ξ, and the sound radiation of accelerating same-sign vortex pairs is modeled by smoothly increasing the dissipation η^* as their separation decreases. During our simulations only 3% of the vortices are lost.
[88] M. T. Reeves, T. P. Billam, B. P. Anderson, and A. S. Bradley, Phys. Rev. A **89**, 053631 (2014).
[89] C. Jones and P. Roberts, J. Phys. A **15**, 2599 (1982).
[90] C. Jones, S. Putterman, and P. Roberts, J. Phys. A **19**, 2991 (1986).
[91] See Supplemental Material at http://link.aps.org/supplemental/10.1103/PhysRevLett.119.185301 for a more detailed discussion, which includes Refs. [21,22,27,79,80,89,94–96].

[92] E. W. Streed, A. P. Chikkatur, T. L. Gustavson, M. Boyd, Y. Torii, D. Schneble, G. K. Campbell, D. E. Pritchard, and W. Ketterle, Rev. Sci. Instrum. **77**, 023106 (2006).

[93] K. M. R. van der Stam, E. D. van Ooijen, R. Meppelink, J. M. Vogels, and P. van der Straten, Rev. Sci. Instrum. **78**, 013102 (2007).

[94] T. W. Neely, A. S. Bradley, E. C. Samson, S. J. Rooney, E. M. Wright, K. J. H. Law, R. Carretero-González, P. G. Kevrekidis, M. J. Davis, and B. P. Anderson, Phys. Rev. Lett. **111**, 235301 (2013); see Supplemental Material for additional information.

[95] P. G. de Gennes and J. Prost, *The Physics of Liquid Crystals* (Clarendon, Oxford, 1993), 2nd ed.